Car-Parrinello molecular dynamics study of a blue-shifted intermolecular weak-hydrogen-bond system

Rodziewicz, P.; Melikova, S.M.; Rutkowski, K.S.; Buda, F.

Car–Parrinello Molecular Dynamics Study of a Blue-Shifted Intermolecular Weak-Hydrogen-Bond System

Pawel Rodziewicz,[c] Sonia M. Melikova,[b] Konstantin S. Rutkowski,[b] and Francesco Buda*[a]

The role played by hydrogen bonds in nature can hardly be overemphasized. Its importance in structures of biological interest has been well documented in numerous papers published since the discovery of this phenomenon.[1] According to a classical definition of the hydrogen bond, an A–H···B system can be described as a donor part A–H interacting with an acceptor B, where A is an electronegative atom and B is either an electronegative atom or a group with a region of a high electron density.[2–4] Standard hydrogen-bond formation is accompanied by a noticeable charge transfer from B to the A–H σ^* antibonding orbital, which causes elongation of the A–H bond.[5] Spectroscopic studies show that the fundamental stretching frequency $\tilde{\nu}$(A–H) is red-shifted, with a corresponding increase in integrated intensity. Among the characteristic features of hydrogen-bond formation, the red shift of the A–H stretching frequency is seen as the most important manifestation of this phenomenon.

Surprisingly, a totally different situation from that described above may occur. First experimental evidence of the so-called blue-shifting hydrogen bond was detected several decades ago.[6–7] Contrary to the red shift of the ν(A–H) stretching frequency, the observed blue shift is often accompanied by a decrease in intensity. Nowadays a variety of systems exhibiting blue shift have been detected in the gas,[8] liquid,[9] and solid states.[10] Several names have been proposed in the literature for this unusual behavior: anti-hydrogen bond,[11] improper,[12] blue-shifting,[13] or blue-shifted hydrogen bond.[14–15] This phenomenon has been mainly reported for C–H bonds, but some theoretical studies also suggest the existence of blue-shifting hydrogen bond in the case of Si–H, P–H, and N–H bonds.[14,16–17] First attempts at a theoretical description of this phenomenon were based on semi-empirical calculations.[18] Though several and often mutually exclusive explanations have been discussed in the literature, a clear picture of the nature of the blue-shift phenomenon has not yet emerged.[19–28]

Here we investigate theoretically a model system consisting of fluoroform dissolved in liquid carbon monoxide at a temperature of 100 K using Car–Parrinello molecular dynamics (CPMD).[29] This system involving weak blue-shifted H-bond interactions was recently investigated experimentally in detail by FTIR spectroscopy.[22] The Car–Parrinello method allows us to follow the dynamics of complex formation and breaking with interactions described at the density functional theory (DFT) level. The stoichiometry of the different complexes and their residence time can be naturally derived. Finally, the analysis of both the Fourier transform of the velocity–velocity and dipole-moment autocorrelation functions enables direct comparison with experimental spectroscopic data.

Results and Discussion

Ab initio and DFT Calculations

The most relevant structural and spectroscopic properties of fluoroform complexes of different stoichiometry obtained with static calculations at the MP2 level are collected in Figure 1. A more detailed description of the complexes is reported in Table 1. All of the found structures exhibit a negative binding energy and a blue shift in the C–H stretching frequency. Fluoroform can interact with either the carbon or the oxygen atom

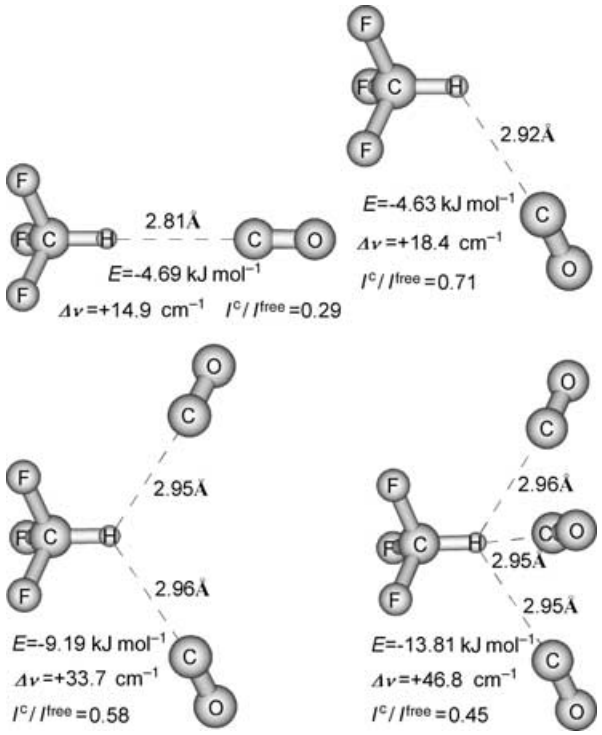

Figure 1. Structures of $F_3CH\cdots CO$ complexes predicted on the basis of MP2-(full)/6-31+G(d, p) calculations using counterpoise-corrected potential-energy surface (PES). For each structure, the H···C distances, the binding energy E [kJ mol^{-1}], the frequency shift $\Delta\tilde{\nu}$ [cm^{-1}] of the ν_1 vibration, and the I^c/I^{free} ratio (where I^c and I^{free} are integrated intensities of the band attributed to the complex and free molecule, respectively) are given.

[a] *Dr. F. Buda*
Leiden Institute of Chemistry, University of Leiden
Einsteinweg 55, 2300 RA Leiden (The Netherlands)
Fax: +(31) 71-5274603
E-mail: f.buda@chem.leidenuniv.nl

[b] *Dr. S. M. Melikova, Dr. K. S. Rutkowski*
Institute of Physics, St. Petersburg State University
Ulianovskaja 1, St. Petersburg, Peterhof, 198504 (Russia)

[c] *P. Rodziewicz*
Faculty of Chemistry, University of Wroclaw
14 F. Joliot-Curie 50-383 Wroclaw (Poland)

Supporting information for this article is available on the WWW under http://www.chemphyschem.org or from the author.

 DOI: 10.1002/cphc.200400577

Table 1. Ab initio structural and spectroscopic parameters of $F_3CH\cdots n\,CO$ complexes predicted at the counterpoise-corrected MP2(full)/6-31+G(d,p) level. Bond lengths are given in Å, angles in degrees. Δr(C–H) is the contraction of the C–H bond length on complexation. Frequencies $\tilde{\nu}_i$ are given in cm^{-1} and intensities I_i in $km\,mol^{-1}$. $\Delta\tilde{\nu}_1$ is the blue shift of the C–H stretching frequency $\tilde{\nu}_1$ on complexation. The ratio I_1^c/I_1^{free} between the integrated intensities of the $\tilde{\nu}_1$ band in the complex I_c and in the monomer I_{free} is also given. E [$kJ\,mol^{-1}$] is the binding energy.

	F_3CH free	CO linear	OC linear	CO bent	OC bent	2 CO	2 OC	CO OC	3 CO	3 OC	2 OC 1 CO	2CO 1OC
r(C–H)	1.0838	1.0832	1.0834	1.0827	1.0834	1.0817	1.0827	1.0823	1.0810	1.0818	1.0820	1.0813
Δr (C–H)	–	0.0006	0.0004	0.0011	0.0004	0.0021	0.0011	0.0015	0.0028	0.002	0.0018	0.0025
$r(C-F_1)$	1.3489	1.3502	1.3493	1.3500	1.3493	1.3508	1.3499	1.3504	1.3516	1.3502	1.3511	1.3512
$r(C-F_2)$	1.3489	1.3502	1.3493	1.3497	1.3492	1.3511	1.3495	1.3503	1.3516	1.3502	1.3505	1.3512
$r(C-F_3)$	1.3489	1.3502	1.3493	1.3499	1.3492	1.3511	1.3495	1.3501	1.3515	1.3502	1.3504	1.3509
$\measuredangle(C\text{-}H\text{-}C_1)$	–	180.0	180.0	123.9	106.8	119.2	113.8	125.4	119.3	127.4	139.0	120.8
$\measuredangle(C\text{-}H\text{-}C_2)$	–	–	–	–	–	119.4	113.8	103.8	119.2	128.2	105.6	120.8
$\measuredangle(C\text{-}H\text{-}C_3)$	–	–	–	–	–	–	–	–	119.1	128.2	115.8	103.4
$\measuredangle(C\text{-}H\text{-}O_1)$	–	180.0	180.0	121.3	111.9	117.2	118.7	124.2	117.4	130.9	138.7	118.8
$\measuredangle(C\text{-}H\text{-}O_2)$	–	–	–	–	–	117.4	118.7	109.6	117.2	131.5	111.8	118.8
$\measuredangle(C\text{-}H\text{-}O_3)$	–	–	–	–	–	–	–	–	117.1	131.5	122.2	109.8
$R(H\cdots C_1)$	–	2.814	3.855	2.915	3.968	2.949	3.910	2.907	2.957	3.852	2.850	2.934
$R(H\cdots C_2)$	–	–	–	–	–	2.957	3.910	3.984	2.949	3.849	3.942	2.935
$R(H\cdots C_3)$	–	–	–	–	–	–	–	–	2.942	3.847	3.898	3.969
$R(H\cdots O_1)$	–	3.963	2.704	4.055	2.857	4.093	2.796	4.052	4.101	2.716	4.000	4.079
$R(H\cdots O_2)$	–	–	–	–	–	4.101	2.796	2.881	4.093	2.712	2.852	4.079
$R(H\cdots O_3)$	–	–	–	–	–	–	–	–	4.086	2.710	2.810	2.881
E	–	−4.69	−2.09	−4.63	−2.49	−9.19	−5.62	−6.97	−13.81	−9.31	−9.99	−11.45
$\tilde{\nu}_1$	3273.0	3287.9	3284.1	3291.4	3281.3	3306.7	3292.1	3298.7	3319.8	3310.2	3306.4	3314.0
I_1	24.9	7.2	14.0	17.8	22.1	14.5	18.7	15.8	11.2	11.7	10.6	12.5
$\Delta\tilde{\nu}_1$	–	+14.9	+11.1	+18.4	+8.3	+33.7	+19.1	+25.7	+46.8	+37.2	+33.4	+41.0
I_1^c/I_1^{free}	–	0.29	0.56	0.71	0.89	0.58	0.75	0.63	0.45	0.47	0.43	0.50
$\tilde{\nu}_2$	1142.6	1139.2	1141.3	1140.6	1141.9	1138.2	1141.0	1139.7	1137.0	1139.7	1138.4	1137.9
I_2	102	127.8	123.0	110.9	103.7	114.9	108.2	111.0	115.7	126.1	118.1	112.0
$\tilde{\nu}_3$	687.5	686.3	686.9	686.7	687.3	685.6	686.8	686.4	685.3	686.1	685.9	685.6
I_3	14.3	17.6	17.0	15.4	14.6	15.9	15.4	15.6	16.7	17.9	16.8	16.1
$\tilde{\nu}_4$	1422.6	1431.3	1427.1	1420.	1421.6	1418.1	1424.0	1420.6	1422.0	1427.8	1423.9	1419.4
		1431.3	1427.1	1427.2	1424.1	1426.4	1424.5	1427.0	1422.4	1427.9	1430.5	1426.3
I_4	118	56.3	57.8	47.3	52.1	40.4	48.4	43.5	38.0	43.0	38.8	37.8
		56.3	57.8	54.6	56.2	47.4	48.5	50.0	38.0	43.3	47.3	42.4
$\tilde{\nu}_5$	1170.9	1166.6	1169.9	1166.9	1169.7	1163.7	1168.2	1166.0	1161.1	1167.9	1164.2	1163.0
		1166.6	1169.9	1168.5	1170.6	1163.8	1170.1	1167.2	1161.5	1167.9	1166.4	1163.8
I_5	633	309.7	310.8	303.5	304.6	328.2	324.1	307.1	321.7	320.0	330.2	324.6
		309.7	310.8	332.6	339.3	312.1	326.5	338.9	322.0	320.4	316.0	325.5
$\tilde{\nu}_6$	497.9	497.6	497.7	497.7	497.9	497.7	497.8	497.9	498.4	497.8	497.8	498.3
		497.6	497.7	498.3	498.4	498.4	498.5	498.4	498.4	497.8	498.2	498.4
I_6	6.3	2.93	3.04	3.00	3.08	3.14	3.47	3.22	3.48	3.40	3.47	3.55
		2.93	3.04	3.54	3.78	3.64	3.55	3.80	3.48	3.40	3.41	3.68

of CO molecules. Therefore, we considered different types of complexes interacting either through carbon or oxygen alone or through a combination of the two. Their stoichiometry varies from 1:1 (F_3CH:CO) to 1:3. A clear trend can be observed (see Table 1), namely, that the binding energy of complexes interacting through oxygen ($F_3CH\cdots OC$) is smaller (by about 2.6 $kJ\,mol^{-1}$) than those interacting through carbon ($F_3CH\cdots CO$). Similarly, for the complexes with 1:2 and 1:3 stoichiometry, the stability increases with increasing number of $F_3CH\cdots CO$ bonds in the complex. The C–H bond contraction and the associated blue shift in the stretching frequency also follow the same trend and become larger with increasing binding energy. The largest C–H bond contraction (−0.0028 Å) and frequency shift (+46.8 cm^{-1}) occur when fluoroform forms a complex with three CO molecules interacting through carbon ($F_3CH\cdots CO,CO,CO$). We found two different types of 1:1 complex: linear and bent. In the case of complexes interacting through the carbon atom, they have almost the same binding energy and differ only slightly in C–H stretching frequency. In contrast, for complexes interacting though oxygen, the bent form is more favorable and the linear form appears to be unstable: one imaginary vibrational mode is detected, which tends to bend the linear structure.

We also performed DFT calculations with different functionals (B3LYP, BLYP) to check whether geometric and spectroscopic parameters are comparable with MP2 results. Table 2 compares MP2 and DFT results for different basis sets for the linear complex $F_3CH\cdots CO$. The contraction of the C–H bond on complex formation and the blue shift of its stretching frequency are correctly reproduced by both MP2 and DFT methods (with B3LYP and BLYP functionals). This finding together with the analysis of the other complexes with different stoichiometry (not reported in Table 2) demonstrates that DFT describes quite well the so-called blue-shift phenomenon, even with the nonhybrid functional BLYP.

Table 2. Predicted structural and spectroscopic parameters of linear $F_3CH\cdots CO$ complex. Bond lengths are given in Å, angles in °. Δr is the bond length change on complexation. Frequencies $\tilde{\nu}$ are given in cm^{-1} and intensities I_i in $km\,mol^{-1}$. $\Delta\tilde{\nu}$ is the blue shift of the C–H stretching frequency $\tilde{\nu}_1$ on complexation. The ratio I_1^c/I_1^{free} between the integrated intensities of the $\tilde{\nu}_1$ band in the complex I_c and in the monomer I_{free} is also given. E [$kJ\,mol^{-1}$] is the binding energy.[a]

	MP2(full)[b] CP	MP2(full)[c] CP PES	DFT/B3LYP[b] CP	DFT/B3LYP[c] CP PES	DFT/BLYP[c] CP PES
r(C–H)	1.0835	1.0832	1.0882	1.0907	1.0981
Δr(C–H)	−0.001	−0.0006	−0.0008	−0.0006	−0.0007
R(C–$F_{1,2,3}$)	1.3312	1.3502	1.3397	1.3490	1.3683
Δr(C–$F_{1,2,3}$)	+0.0017	+0.0013	+0.0013	+0.0013	+0.0013
$\tilde{\nu}_1$	3227.0	3287.9	3142.0	3176.6	3086.0
$\Delta\tilde{\nu}$	+27.0	+14.9	+15	+13.1	+13.0
I_1	2.8	7.2	5.4	6.1	5.2
I_1^c/I_1^{free}	0.117	0.289	0.193	0.222	0.191
E	−6.7	−4.7	−2.9	−3.2	−2.7
R(H···C)	2.619	2.814	2.758	2.786	2.831
∢(CH–C)	180.0	180.0	180.0	180.0	180.0

[a] CP = counterpoise correction used only for the equilibration structure, CP PES = counterpoise correction used both in geometry optimization and calculation of frequency. [b] 6-311++G(3df, 3pd). [c] 6-31+G(d,p).

Car–Parrinello Molecular Dynamics Simulation

The most characteristic feature of the improper hydrogen bond is the blue shift and decreased intensity of the C–H stretching band. Table 3 lists the frequencies derived from the CPMD simulations by using the velocity–velocity and the dipole-moment autocorrelation functions. For comparison we also show the experimental frequencies for fluoroform in the gas phase[30–31] and in carbon monoxide solution[22] at 100 K. The CPMD simulation correctly predicts the blue shift $\Delta\tilde{\nu}_1$ (+27 cm^{-1}), albeit overestimated by 10 cm^{-1} in comparison to experiment. Also the intensity of the peak attributed to this band decreases in qualitative agreement with experiment. These results demonstrate that CPMD is a reliable method for describing systems with unusual hydrogen bonds. The CPMD results for other vibrational bands also reveal a reasonable agreement with experimental data. In particular, the symmetric and asymmetric C–F stretching frequencies ($\tilde{\nu}_2$ and $\tilde{\nu}_5$) are correctly predicted to be red-shifted, while the C–H bending frequency ($\tilde{\nu}_4$) is basically unchanged within the statistical error, in line with the very small experimental shift (see Table 3). The vibrational analysis of the solvated fluoroform simulation shows a peak at 1866 cm^{-1} that is ascribed to the CO stretching vibration.

Table 3. Comparison between experimental and computed frequencies [cm^{-1}] for F_3CH in the gas phase and in liquid CO at 100 K. The frequency shift $\tilde{\nu}_{c\text{-}g}$ between the liquid and the gas phase is also given.

Assignment (Symmetry)	Experimental FTIR data[22]			Theoretical results (CPMD)		
	F_3CH, gas phase	F_3CH in liquid CO, 100 K		F_3CH, gas phase	F_3CH in liquid CO, 100 K	
	$\tilde{\nu}_g$	$\tilde{\nu}_c$	$\tilde{\nu}_{c\text{-}g}$	$\tilde{\nu}_g$	$\tilde{\nu}_c$	$\tilde{\nu}_{c\text{-}g}$
$\tilde{\nu}_2$ (A_1) sym. C–F str.	1141.5	1136.0	−5.5	1026	1021	−5
$\tilde{\nu}_5$ (E) asym. C–F str.	1158.3	1142.0	−16.3	1047	1037	−10
$\tilde{\nu}_4$ (E) C–H bend.	1377.9	1376.0	−1.9	1260	1260	0
$\tilde{\nu}_1$ (A_1) C–H str.	3035.2	3052.3	+17.3	2840	2867	+27

Another important manifestation of formation of the blue-shifted complex is a contraction of the C–H bond of the proton-donor molecule, which corresponds to an increase in the force constant. The static calculations discussed above predict a variety of contraction values that depend on the stoichiometry of the complex. In the molecular dynamics simulation this contraction can be calculated as the difference between the expectation value of the C–H bond length in the simulation of F_3CH dissolved in CO and the same expectation value in the run of F_3CH in vacuum. We obtained a contraction of 0.002 Å (±0.0002 Å) for the C–H bond length of F_3CH on interaction with CO molecules. In the CPMD run we also observed lengthening of the C–F bond, in agreement with static ab initio and DFT calculations.

The CPMD simulation also gives relevant information about the nature and structure of the dynamically forming and breaking complexes. Figures 2 and 3 show two-dimensional histograms representing the probability of finding a complex with a given C···H or O···H distance (R(C···H,O···H) = 2.2–4.0 Å) and C–H···C or C–H···O angle (∢(C–H···C,C–H···O) = 90–180°), respectively. With this choice of structural parameters we can study the mutual orientation of CO molecules with respect to the F_3CH solute. Particular colors in Figures 2 and 3 refer to the number of complexes with a particular distance and angle that occurred during the CPMD run. We report only the angles ∢(C–H···C(O) between 90 and 180°, since we do not observe the formation of complexes with angles less than 90°.

We concentrate our analysis on distances between the H atom of F_3CH and C or O of CO molecules in the range 2.6–3.0 Å. This corresponds to the typical distances in complex formation according to the static calculations (see Figure 1). A first comparison between Figures 2 and 3 shows that interaction with oxygen is less probable than with carbon. This result is in line with static DFT and ab initio calculations predicting larger binding energy for the structure in which the C atom of CO is nearest to the H atom of F_3CH. In Figure 3 we observe clear peaks corresponding to angles ∢(C–H···O) = 145, 110° and distances R(H···O) = 2.5, 2.8 Å, respectively. Thus, complex formation with oxygen as binding atom occurs in a bent structure. No linear complex is observed. Since the average CO

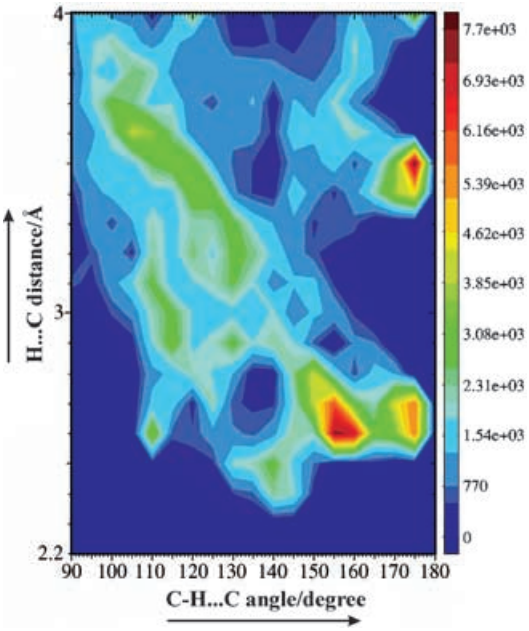

Figure 2. Number of configurations detected along the CPMD simulation with a given H···C distance (H of F_3CH and C of all CO molecules) and C–H···C angle.

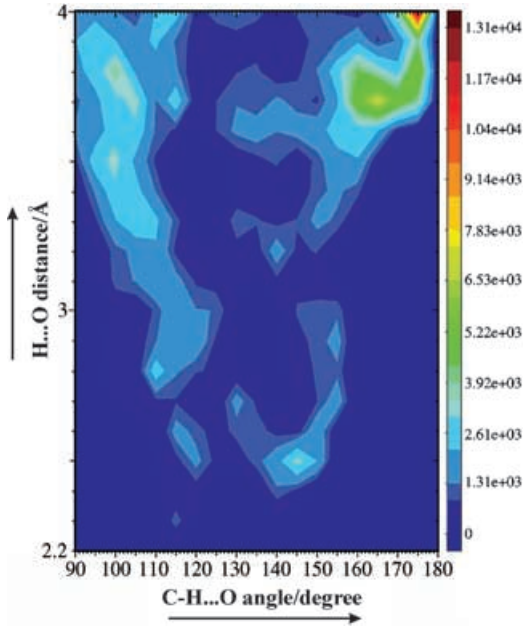

Figure 3. Number of configurations detected along the CPMD simulation with a given H···O distance (H of F_3CH and O of all CO molecules) and C–H···O angle.

bond length is on the order of 1.2 Å, a peak corresponding to the carbon atom in this F_3CH···OC complex can be found in Figure 2 in the region R(H···C) = 3.3–3.7 Å, $\sphericalangle$(C–H···C) = 100–110°.

Analyzing the area of the closest possible interaction between the carbon atom of CO and the F_3CH molecule in Figure 2, we observe peaks at the positions (2.6 Å, 175°), (2.6 Å, 155°), and (2.6 Å, 110°). Therefore, also in this case bent complexes are predominant. Though there is no clear evidence of linear complexes, we observe the formation of complexes with larger angles $\sphericalangle$(C–H···C) = 150–175° than in the case of oxygen as a binding atom. The corresponding O atom in this last type of complexes can be associated with the peak at (3.7 Å, 165°) in Figure 3.

On the basis of the CPMD trajectory we conclude that dynamical effects tend to favor the formation of bent complexes over linear ones. This result is in contrast with static calculations, which give the same binding energy for bent and linear F_3CH···CO complexes.

From the analysis of the MD trajectory we can also extract information about the stoichiometry of the formed complexes and their residence time. The stoichiometry of the complexes was calculated as the number of C or O atoms of CO molecules whose distance from the H atom of F_3CH is within an interaction distance of 3 Å at each step of the MD. In a similar way the residence time τ was estimated as the time period in which either C or O is within the sphere defined by R(C–H···C(O)) = 3 Å. Of course a different choice of R(C–H···C(O)) would also influence the estimated residence time. Plots of all H···C and H···O distances versus time during the CPMD simulation are available as Supporting Information (Figures S1 and S2). We find that binding of the F_3CH molecule with only one CO molecule in solution is noticeably more preferable in such a weak hydrogen-bond system. Both F_3CH···CO and F_3CH···OC complexes have lifetimes on the order of 150 fs. Complexes with stoichiometry higher than 1:1 occur less frequently. Within our limited statistics, we can conclude that the lifetime of complexes with more than one CO molecule is two or three times shorter than in the case of 1:1 complexes [$\tau \approx 80$ fs (F_3CH···CO,CO), 60 fs (F_3CH···OC,OC), 50 fs (F_3CH···OC,CO)]. The relatively short residence time of different types of complexes is consistent with the rather small binding energy. Nevertheless, the ratio between the total time in which at least one type of complex is formed and the total length of the simulation is about 66%. If we consider separately the different complexes, we find that the F_3CH···CO complex occurs more frequently (ca. 35% of the total time) followed by the F_3CH···OC complex (ca. 19%).

Conclusions

We have presented a Car–Parrinello molecular dynamics study of the interaction between fluoroform and carbon monoxide molecules in the liquid phase at 100 K. We have confirmed that this system can be characterized as a blue-shifted weak hydrogen-bond system. Contrary to a standard definition of the hydrogen bond and in agreement with experimental (FTIR) data, our simulation gives a blue-shifted fundamental stretching frequency $\tilde{\nu}$(C–H) and a decrease in the corresponding integrated intensity. Moreover, the interaction of F_3CH with CO molecules leads to contraction of the C–H bond. The analysis of the trajectory provides an insight into the nature, structure, and lifetime of the complexes formed in the liquid that is not accessible from static calculations. The most frequently observed complex is the F_3CH···CO with a bent geometry.

Computational Methods

All static, ab initio, and DFT calculations were performed with the Gaussian 98 package.[32] The ab initio calculations were performed at the MP2 level, which generally provides an accurate description of hydrogen bonds. For the DFT calculations both BLYP[33–34] and B3LYP[35] functionals were used. Geometry optimization was done without any constraint and each optimized structure was checked to be a real minimum by a frequency calculation. The energies of the studied complexes are relatively small and the basis set superposition error (BSSE) could significantly influence their geometry.[36–37] Therefore, the counterpoise (CP) method was chosen during geometry optimization and in the normal-mode analysis.[38] Most of the calculations were carried out with a 6-31++G(d,p) basis set. In a few cases we used the larger 6-311++G(3df,3pd) basis set to check the convergence of the results. It is often suggested that the application of diffuse functions and multiple sets of polarization functions, both on hydrogen and heavy atoms, may be of crucial importance when studying effects of weakly bound complex formation.[39]

The first-principles molecular dynamics simulations were performed by using the Car–Parrinello approach as implemented in the CPMD program.[40] This is a well-established tool for investigating liquid and disordered systems and it has been applied to a variety of problems, including hydrogen-bonded systems and chemical reactions in water.[41–45] In the CPMD runs we used the gradient-corrected BLYP exchange-correlation functional.[33–34] This choice is justified by static test calculations showing that the BLYP functional properly describes the unusual blue-shift effect in hydrogen-bond formation (see Table 2). We simulated a system consisting of a single fluoroform molecule and 26 carbon monoxide molecules in a cubic cell of side $a = 11.2$ Å with periodic boundary conditions at a temperature of 100 K. The concentration of fluroroform, the density of the solution, and the temperature were set up according to the experimental conditions.[22] A simulation of a single fluoroform molecule in vacuum was performed under the same conditions in a box of the same size. We used pseudopotentials in the form proposed by Hartwigsen et al.[46] with a plane-wave energy cutoff of 60 Ry. Test calculations performed for isolated fluoroform using different energy cutoffs proved that a value of 60 Ry is a good compromise between efficiency and quality in the description of the system. For the molecular dynamics we took a time step of 5 a.u. and a fictitious electronic mass of 400 a.u. The system was equilibrated under NVT conditions for 7 ps before accumulating statistics for an additional period of 5 ps. Autocorrelation functions were calculated using the TISEAN package.[47] Frequencies and IR intensities were generated from the Fourier transform of the velocity and dipole-moment autocorrelation functions.[41] The two-dimensional histograms shown in Figures 2 and 3 were normalized per unit solid angle by using a geometrical correction factor, as is usually done in analysis of H bonds.[48]

Acknowledgements

P.R. gratefully acknowledges Prof. Gerhard Stock and Dr Daniil Kosov for fruitful discussions and their hospitality during the stay in Frankfurt am Main in 2003. P.R. also acknowledges support by KBN (Grant No 3 T09A 158 27).

Keywords: ab initio calculations · autocorrelation functions · density functional calculations · hydrogen bonds · molecular dynamics

[1] W. M. Latimer, W. H. Rodebush, *J. Am. Chem. Soc.* **1920**, *42*, 1419–1433.
[2] S. Scheiner, *Hydrogen Bonding. A Theoretical Perspective*, Oxford University Press, Oxford, **1997**.
[3] G. Desiraju, G. R. Steiner, *The Weak Hydrogen Bond*, Oxford University Press, Oxford, **1999**.
[4] G. Jeffrey, *An Introduction to Hydrogen Bonding*, Oxford University Press, New York, **1997**.
[5] T. Steiner, *Angew. Chem.* **2002**, *114,* 50–80; *Angew. Chem. Int. Ed. Engl.* **2002**, *41*, 48–76.
[6] N. S. Golubev, T. D. Kolomiitsova, S. M. Melikova, D. N. Shchepkin, *18th Conference on Spectroscopy*, Technical Digest, Gorki, Russia, **1977**, p. 78.
[7] M. O. Bulanin, T. D. Kolomiitsova, V. A. Kondaurov, S. M. Melikova, *Opt. Spectrosc. (Russ.)* **1990**, *68*, 763.
[8] B. Reimann, K. Buchhold, S. Vaupel, B. Brutschy, *Z. Phys. Chem.* **2001**, *215*, 777.
[9] V.V. Bertcev, N. S. Golubev, D. N. Shchepkin, *Opt. Spectrosc. (Russ.)* **1977**, *40*, 951.
[10] K. A. Wickersheim, *J. Chem. Phys.* **1959**, *31*, 863.
[11] P. Hobza, Z. Havlas, *Chem. Phys. Lett.* **1999**, *303*, 447–452.
[12] P. Hobza, Z. Havlas, *Chem. Rev.* **2000**, *100*, 4253.
[13] H. Matsuura, H. Yoshida, M. Hieda, S. Yamanaka, T. Harada, K. Shin-ya, K. Ohno, *J. Am. Chem. Soc.* **2003**, *125*, 13911.
[14] X. Li, L. Liu, H. B. Schleger, *J. Am. Chem. Soc.* **2002**, *124*, 9639.
[15] A. Karpfen, E. Kryachko, *J. Phys. Chem. A* **2003**, *107*, 9724.
[16] Y. Fang, J.-M. Fan, L. Liu, X.-S. Li, Q.-X. Guo, *Chem. Lett.* **2002**, *1,* 116.
[17] J. M. Fan, L. Liu, Q.-X. Guo, *Chem. Phys. Lett.* **2002**, *365*, 464.
[18] I. E. Boldeskul, I. F. Tsymbal, E. V. Ryltsev, Z. Latajka, A. J. Barnes, *J. Mol. Struct.* **1996**, *436*, 167.
[19] Y. Tatamitani, B. Liu, J. Shimada, T. Ogata, P. Ottaviani, A. Maris, W. Caminati, J. L. Alonso, *J. Am. Chem. Soc.* **2002**, *124*, 2739.
[20] B. J. van der Veken, W. A. Herrebout, R. Szostak, D. N. Shchepkin, Z. Havlas, P. Hobza, *J. Am. Chem. Soc.* **2001**, *123*, 12290.
[21] Y. Gu, T. Kar, S. Scheiner, *J. Am. Chem. Soc.* **1999**, *121*, 9411.
[22] S. M. Melikova, K.S Rutkowski, P. Rodziewicz, A. Koll, *Chem. Phys. Lett.* **2002**, *352*, 301.
[23] K. Hermansson, *J. Phys. Chem. A* **2002**, *106*, 4695.
[24] L. Pejov, K. Hermansson, *J. Chem. Phys.* **2003**, *119*, 313.
[25] I. V. Alabugin, M. Manoharan, S. Peabody, F. Weinhold, *J. Am. Chem. Soc.* **2003**, *125*, 5973.
[26] E. Mrazkova, P. Hobza, *J. Phys. Chem. A* **2003**, *107*, 1032–1039.
[27] I. V. Alabugin, M. Manoharan, F. Weinhold, *J. Phys. Chem. A* **2004**, *108*, 4720.
[28] A. J. Barnes, *J. Mol. Struct.* **2004**, *704*, 3
[29] R. Car, M. Parrinello, *Phys. Rev. Lett.* **1985**, *55*, 2471
[30] J. Segall, R. N. Zare, H. R. Dubal, M. Lewerenz, M. Quack, *J. Chem. Phys.* **1987**, *86*, 634.
[31] H. R. Dubal, T. K. Ha, M. Lewerenz, M. Quack, *J. Chem. Phys.* **1989**, *91*, 6698.
[32] Gaussian 98 (revision A.11.1), M. J. Frisch, G. W. Trucks, H. B. Schlegel, G. E. Scuseria, M. A. Robb, J. R. Cheeseman, V. G. Zakrzewski, J. A. Jr., Montgomery, R. E. Stratmann, J. C. Burant, S. Dapprich, J. M. Millam, A. D. Daniels, K. N. Kudin, M. C. Strain, O. Farkas, J. Tomasi, V. Barone, M. Cossi, R. Cammi, B. Mennucci, C. Pomelli, C. Adamo, Clifford., J. Ochterski, G. A. Peterson, P. Y. Ayala, Q. Cui, K. Morokuma, P. Salvador, J. J. Dannenberg, D. K. Malick, A. D. Rabuck, K. Raghavachari, J. B. Foresman, J. Cioslowski, J.V. Ortiz, A. G. Baboul, B. B. Stefanov, G. Liu, A. Liashenko, P. Piskorz, I. Komaromi, R. Gomperts, R. L. Martin, D. J. Fox, T. Keith, M. A. Al-Laham, C. Y. Peng, A. Nanayakkara, M. Challacombe, P. M. W. Gill, B. Johnson, W. Chen, M. W. Wong, J. L. Andres, C. Gonzalez, M. Head-Gordon, E. S. Replogle, J. A. Pople, Gaussian, Inc., Pittsburgh, PA, 2001.
[33] A. D. Becke, *Phys. Rev. A* **1988**, *38*, 3098.
[34] C. Lee, W. Yang, R. G. Parr, *Phys. Rev. B* **1988**, *37*, 785.
[35] A. D. Becke, *J. Chem. Phys.* **1993**, *98*, 5648.
[36] P. Salvador, M. Duran, *J. Chem. Phys.* **1999**, *111*, 4460.
[37] S. Simon, M. Duran, J. J. Dannenberg, *J. Chem. Phys.* **1996**, *105*, 11024.
[38] S. F. Boys, F. Bernardy, *Mol. Phys.* **1970**, *19*, 553.
[39] Th. H. Dunning, Jr., K. A. Peterson, D. E. Woon, *Basis Sets: Correlation Consistent Sets in Encyclopedia of Computational Chemistry, Vol.* 1 (Eds.: P. v. R. Schleyer, N. L. Allinger, T. Clark, J. Gasteiger, P. A. Kollman, H. F. Schaefer, P. R. Shreiner), Wiley, Chichester, **2000**.

[40] CPMD V3.7, Copyright IBM Corp **1990–2003**, Copyright MPI für Festkoerperforschung, Stuttgart **1997–2001**.
[41] P. L. Silvestrelli, M. Bernasconi, M. Parrinello, *Chem. Phys. Lett.* **1997**, *277*, 478.
[42] S. Izvekov, G. A. Voth, *J. Chem. Phys.* **2002**, *116*, 10372.
[43] M. Pagliai, S. Raugei, G. Cardini, V. Schettino, *J. Mol. Struct. (THEOCHEM)* **2003**, *630*, 141.
[44] B. L. Trout, B. H. Suits, R. J. Gorte, D. White, *J. Phys. Chem. B* **2000**, *104*, 11734.
[45] B. Ensing, F. Buda, M. C. M. Gribnau, E. J. Baerends, *J. Am. Chem. Soc.* **2004**, *126*, 4355–4365.
[46] C. Hartwigsen, S. Goedecker, J. Hutter, *Phys. Rev. B* **1998**, *58*, 3641–3662
[47] R. Hegger, H. Kantz, T. Schreiber, *CHAOS* **1999**, *9*, 413
[48] I. Olovsson, P. G. Jönsson in *The Hydrogen Bond. Recent Developments in Theory and Experiments*, *Vol.* 2 (Eds.: P. Schuster, G. Zundel, C. Sandorfy), North-Holland Publishing Company, Amsterdam, **1976**, pp. 393–456.

Received: November 30, 2004
Published online on August 5, 2005

